

Research Article

Phosphorylation of p27^{BBP}/eIF6 and its association with the cytoskeleton are developmentally regulated in *Xenopus* oogenesis

R. Carotenuto^a, N. De Marco^a, S. Biffo^b, M. Wilding^c, M. C. Vaccaro^a, P. C. Marchisio^d, T. Capriglione^a, G. L. Russo^e and C. Campanella^{a,*}

^a Dipartimento di Biologia Strutturale e Funzionale, Università di Napoli Federico II, Napoli (Italy), Fax + 39 081 2535035, e-mail: chiara.campanella@unina.it

^b Dipartimento di Scienze dell'Ambiente e della Vita, Università del Piemonte Orientale, Alessandria (Italy)

^c Centro per la Biologia della Riproduzione, Clinica Villa del Sole, Napoli (Italy)

^d DIBIT e Università Vita-Salute San Raffaele Milano, (Italy)

^e CNR, Istituto Scienze dell'Alimentazione Avellino (Italy)

Received 7 April 2005; received after revision 11 May 2005; accepted 25 May 2005

Online First 30 June 2005

Abstract. p27^{BBP}/eIF6 is an evolutionarily conserved regulator of ribosomal function. It is necessary for 60S biogenesis and impedes improper joining of 40S and 60S subunits, regulated by protein kinase C or Efl1p. No data on p27^{BBP}/eIF6 during early development of Metazoa are available. We studied the distribution, post-translational changes and association with the cytoskeleton of p27^{BBP}/eIF6 during *Xenopus* oogenesis and early development. Results indicate that p27^{BBP}/eIF6 is present throughout oogenesis, partly associated with 60S subunits, partly free and with little cytoskeleton bound. During prophase I, p27^{BBP}/eIF6 is detected as a single band of 27-kDa. Upon maturation induced by progesterone or protein kinase C, a serine-phosphorylated 29 kDa isoform appears and

is kept throughout development to the neurula stage. Confocal microscopy showed that the distribution of p27^{BBP}/eIF6 and its association with the cytoskeleton varies according to oogenesis stages. Briefly, in stage 6 oocytes, p27^{BBP}/eIF6 has a limited dot-like distribution, and does not co-localize with cytokeratin, whereas upon maturation it spreads throughout the cytoplasm. After fertilization, a large fraction coalesces around cytomembranes and a cytochalasin B-sensitive co-localization with cytokeratin occurs. RNase removes p27^{BBP}/eIF6 from the cytokeratin fibres. Developmental data suggest a role of p27^{BBP}/eIF6 in controlling ribosomal availability or regulating cross-talk between ribosomes and the cytoskeleton.

Key words: *Xenopus*; meiosis; oocyte; 60S; p27^{BBP}/eIF6; phosphorylation; cytokeratin.

The protein p27^{BBP}/eIF6 is an evolutionarily conserved factor necessary for 60S biogenesis in yeast and mammals [1–3]. It is partly associated with 60S and nucleolus associated in all cells [1, 4]. p27^{BBP}/eIF6 was recently shown to prevent improper joining of the 40S and 60S subunits for 80S assemblage [5]. This activity is regulated by Efl1p

in yeast [6] and by protein kinase c (PKC) phosphorylation in mammalian cells [5]. Biochemical work has shown that p27^{BBP}/eIF6 can also bind to β 4 integrin [1, 2]. Although in β 4 integrin-expressing epithelial cells, p27^{BBP}/eIF6 is present at the hemidesmosomes, its ability to associate with intermediate filaments in the nuclear matrix is independent of β 4. No data are available for multicellular organisms, in vivo, during their functional and/or developmental changes. Studies on the in vivo localization of

* Corresponding author. R. Carotenuto and N. De Marco contributed equally to the paper

p27^{BBP}/eIF6 in a developing system may help to evaluate its role and the significance of its association with the cytoskeleton (CSK) and/or phosphorylation.

In this paper, p27^{BBP}/eIF6 was studied in *Xenopus laevis* oogenesis and early development. This model, where $\beta 4$ is lacking [7], has a differentiation program in which both the timing of translation and that of CSK organization are known. Moreover, the *Xenopus* oocyte is among the cells with the largest amount of ribosomes. During oocyte meiosis, two major changes governed by PKC activation occur [8, 9]: the first meiotic reactivation with germinal vesicle breakdown (prophase-metaphase I transition), and the second reactivation after fertilization (metaphase II-telophase II transition). In prophase I oocytes, large amounts of ribosomes accumulate and translation is blocked [10–14]. Blocks are removed by progesterone at maturation when translation increases [see ref. 15].

The CSK also changes during oogenesis and development. In the germinal vesicle, cytoskeletal proteins are found among nucleoli [16, 17]. The oocyte membrane and cytoplasm are characterized by a rich actin-based cytoskeleton. Vimentin and cytokeratin are found in bundles at the peripheral cytoplasm and in radii spanning the cytoplasm [see refs. 18, 19]. Following germinal vesicle breakdown at maturation, the phosphorylation cascade disrupts this organization. Later, in fertilized eggs, the cytokeratin assembles back into peripheral fibres, starting from the vegetal half, together with a thin network throughout the blastomere periphery and cytoplasm [8, 9, 20–23].

In this paper, the data indicate that post-translational changes and distribution of p27^{BBP}/eIF6 are regulated during oogenesis and early development. Following treatment with progesterone or with the tumour-promoting agent (TPA), a serine-phosphorylated form of p27^{BBP}/eIF6 was detected, indicating that at the first meiosis resumption, p27^{BBP}/eIF6 acquires a potential role in protein synthesis regulation. The distribution of p27^{BBP}/eIF6 changes concomitantly with the CSK reorganization that follows maturation and fertilization. Accordingly, data show that after fertilization, p27^{BBP}/eIF6 associates with the CSK.

Materials and methods

Animals

Adult *X. laevis* females were obtained from 'Rettili' Varese, Italy. They were kept and utilized at the Department of Structural and Functional Biology, University of Naples, Federico II, according to the guidelines and policies dictated by the University Animal Welfare Office and in agreement with international rules.

Oocytes at various stages of oogenesis were excised from the ovaries of females anaesthetized with MS222 (Sigma St. Louis, M.). The *X. laevis* oocyte growth stages (Dumont) are: st. 1 (50–300 μm); st. 2 (300–450 μm); st. 3

(450–600 μm); st. 4 (600–1000 μm); st. 5 (1000–1200 μm); st. 6 (1200–1300 μm). Previtellogenic oocytes (sts 1–2) have a large centrally-located germinal vesicle. A flat monolayer of follicle cells surrounds the oocyte, projecting thin villi (macrovilli) in the highly folded oocyte surface. Larger oocytes are vitellogenic and acquire polarization of their constituents. Pigment marks the animal hemisphere where the germinal vesicle is located. The oocytes, surrounded by follicle cells and thecae over the vitelline envelope, represent a functional unit, the follicle.

To obtain eggs, *X. laevis* females were injected in the dorsal lymphatic sac with 500 units of Profasi HP (Serono, Rome, Italy) in Amphibian Ringer (111 mM NaCl, 1.3 mM CaCl₂, 2 mM KCl, 0.8 mM MgSO₄, 25 mM Hepes, pH 7.8). Fertilized eggs, embryos at 2–4 blastomeres and at neurula stage (st. 19, Nieuwkoop and Faber) were obtained by standard in vitro insemination methods.

Antibodies

p27^{BBP}/eIF6 immunostaining was revealed with a rabbit polyclonal antiserum previously described [1], or with a mouse monoclonal recognizing an epitope between amino acids 135 and 200. Rabbit antibodies against the ribosomal protein L5 were prepared as in Nadano et al. [24] and utilized at 1:200 (v/v) dilution. Anti-pan-cytokeratin monoclonal antibody (Sigma C2931), cross-reacting with type I cytokeratin (K18) and type II cytokeratins (K8) of *Xenopus* oocytes [see ref. 25] and polyclonal rabbit anti-phosphoserine (Zymed Laboratories, San Francisco, Calif.) were also utilized at 1:200 (v/v) dilution.

For Western blots of maturation markers, polyclonal rabbit antibody against *Xenopus* Mos (anti-XeMos antibody Sc-86; Santa Cruz Biotechnology, Heidelberg, Germany) and anti-phospho-MAP kinase monoclonal antibody (9106S; New England Biolabs, Beverly, Mass.) were both used at 1:1000 (v/v) dilution.

Sample preparation for SDS-PAGE and Western blot

Oocytes and embryos (neurula stage) were homogenized in a HEPES buffer pH 7.5 containing 900 mM glycerol, 0.02 mM NaN₃, 1 mM ATP, 1 mM DTT, 5 mM EGTA (buffer I) and the following protease inhibitors (Sigma): 2 mM TAME, 5 mg/ml SBTI, 5 $\mu\text{g}/\text{ml}$ aprotinin and 10 μM E64. Unfertilized and fertilized (about 1 h after insemination) eggs were similarly homogenized following removal of the vitelline envelope and the jelly coats. For Maturation Promoting Factor (MPF) activity assays, oocytes were homogenized in buffer I without ATP and containing phosphatase inhibitors (2 mM NAF, 50 mM β -glycerol-phosphate, 1 mM sodium vanadate), in addition to a cocktail of protease inhibitors. After centrifugation at 15,000 g for 40 min at 4°C, protein concentration was determined in the supernatants with the BCA protein assay reagent (Pierce, Rockford, Ill.). After boiling in sample buffer with β -mercaptoethanol, aliquots of 30–60 μg of

proteins were analysed through SDS PAGE (10, 12 or 15% polyacrylamide), utilizing molecular mass standards (200, 116, 97, 45, 31, 21 or 14 kDa) (Bio-Rad, Hercules, Calif.). Oocytes for anti-p27^{BBP}/eIF6 and anti-XeMos/anti-p42/44MAP kinase Western blots were separated on 4–12% NuPage precast gradient gels (Invitrogen, Life Technologies, Carlsbad, Calif.), using Invitrogen SeeBlue plus 2 pre-stained Mr standards (188, 98, 62, 38, 28, 17, 14, 6 or 3 kDa). Proteins were detected by Coomassie staining. Western blotting on nitrocellulose membrane was performed as previously reported [26], using alkaline phosphatase (AP)-conjugated antibodies. Blotting was also performed on Millipore Immobilon-P transfer membrane (Millipore, Bedford, Mass.), utilizing Protein A-peroxidase-linked and chemiluminescence (ECL) Western Blotting Detection Reagent (Amersham Biosciences, Little Chalfont, UK). In some experiments, the same Immobilon-P membrane was used again after exposure to Restore Western Blot Stripping Buffer (Pierce). For Mos and MAP kinase detection, the membranes were incubated with anti-XeMos or with anti-phospho-MAP kinase antibodies, followed by incubation with anti-rabbit or anti-mouse horseradish peroxidase-conjugated IgGs, respectively (Amersham Biosciences).

In vitro maturation Cdc2 and MAP kinase assays

To induce maturation, stage 6 oocytes were excised from the ovaries and de-theated in low-strength saline Steinberg's solution (58 mM NaCl, 0.67 mM KCl, 0.3 mM Ca(NO₃)₂, 0.8 mM MgSO₄, 4.6 mM Tris-HCl pH 7.4). Aliquots of 50 oocytes were incubated for 10–60 min in 32 μM progesterone in OR2 (82.5 mM NaCl, 2.5 mM KCl, 1 mM CaCl₂, 1 mM Na₂HPO₄, 1 mM MgCl₂, 5 mM Hepes, 3.8 mM NaOH, pH 7.4). Similarly, about 50 oocytes were exposed to 150 nM TPA (Sigma) in Ringer (TPA stock solution in DMSO) up to 6 h. As controls, 50 oocytes were incubated in OR2 or in 0.3 M DMSO in Ringer. About 95% of oocytes matured following progesterone treatment, and 78% of oocytes as a result of TPA exposure. Oocytes were also sampled at increasing times following progesterone treatment (0 h; 2 h; 3.5 h; 6 h; 16 h), white spot occurring about 6 h after hormone exposure. Disappearance of the germinal vesicle was also checked by dissecting the oocytes before homogenization. Moreover, previous experimentation showed that about 14 h following 'white-spot' appearance the oocytes are at M-II stage [27]. For staging the progesterone-induced signalling cascade, MPF kinase and MAP kinase activities were assayed. Here some informations about Cdc2 kinase (the catalytic subunit of MPF), *mos* RNA, Mos kinase. Cdc2 kinase, peaks in metaphase I (M-I) and metaphase II (M-II). Translation of maternal *mos* RNA begins shortly after progesterone addition and is maximal in the mature oocyte. Mos kinase starts a phosphorylation cascade leading to the activation of MAP kinase [see ref.

28]. MPF kinase activity was determined by measuring the enzymatic activity of Cdc2 [see ref. 29]. The radioactivity incorporated in the peptide substrate was determined using phosphocellulose paper (Whatman P81). MAP kinase (p42/44MAP kinase; Amersham Biosciences kit RPN84) was assayed following the manufacturer's instructions with some modifications. Briefly, 5 μl of cell lysate (corresponding to 20 μg of total proteins) were added to a reaction mixture containing 10 μl of substrate buffer and 15 μl of [γ -³²P]ATP (50 μM; 5,000 cpm/pmol). The reaction was incubated for 60 min at 30°C, and the amount of phosphorylated peptide was determined as for the Cdc2 kinase assay.

Cytochalasin treatment

Two-cell embryos were exposed to 20 or 50 μM cytochalasin B for 90 min and processed for confocal microscopy parallel to control embryos. Early studies showed that tritiated cytochalasin B does not penetrate into the *Xenopus* egg before first cleavage and cytochalasin B enters the eggs through the unpigmented surface area in the furrow [see ref. 30]. Exposure to the drug was preferred to injection into the egg as it allows an even distribution of the drug in the cell.

Immunoprecipitation

Samples were homogenized in buffer I with the addition of 100 mM NaF and a protease inhibitor cocktail (Sigma P8340), prior to centrifugation at 15,000 g for 45 min. Alternatively, 20 mM Tris-HCl 7.5, 20 mM NaCl, 0.1% NP-40, 10% glycerol and protease inhibitors (buffer II) were used as homogenization buffer. The A431 cell line was used as positive control. Undiluted polyclonal anti-p27^{BBP}/eIF6 or preimmune serum was exposed to supernatants (1:75 v/v) for 1 h under constant agitation. Protein A-Sepharose Cl4B (Pharmacia Biotech) was added to the sample (1:3 v/v) and kept under agitation for 30 min. Following several rinses in buffer I, the recovered precipitates were boiled in sample buffer under reducing conditions.

Phosphatase treatment

Eggs were homogenized in buffer II with the addition of 100 mM phosphatase inhibitor NaF (Sigma P8340), prior to centrifugation. Supernatants containing 600 μg of proteins were immunoprecipitated with polyclonal anti-p27^{BBP}/eIF6 or preimmune serum, for 1 h under constant agitation and exposed to Protein A-Sepharose Cl4B as indicated above. Following several rinses in buffer II, without NaF, the recovered precipitates were suspended in phosphatase buffer (10 mM Tris-HCl, pH 8.5 at 37°C, 10 mM MgCl₂) and treated with 4 U of calf intestinal alkaline phosphatase (New England Biolabs) for 30 min, at room temperature. After treatment and rinsing, beads were resuspended in sample buffer before electrophoresis.

Sucrose gradients

Sucrose gradients were performed according to Ceci et al. [5], modified by a short centrifugation to avoid yolk interference as in Cardinali et al. [31].

Confocal microscopy

Small clusters of previtellogenic oocytes were fixed in 2–4% paraformaldehyde in PBS and extracted in a Hepes buffer containing glycol hexylene [20]. Fully grown oocytes, eggs, fertilized eggs and two-cell embryos were similarly fixed in paraformaldehyde in PBS, omitting the extraction step, according to Gard et al. [18]. The samples were bisected along the equator to separate animal and vegetal halves for the optimization of antibody penetration. All the samples were incubated in anti-p27^{BBP}/eIF6 or in anti-pan-cytokeratin, using rabbit IgG as controls for the purified antibody and PBS for monoclonal antibody. The secondary antibodies were BODIPY FL-conjugated

anti-rabbit goat IgG for anti-p27^{BBP}/eIF6 and Texas Red-conjugated anti-mouse goat antibodies for anti-pan-cytokeratin. For double localization, the samples were incubated with anti-p27^{BBP}/eIF6 and anti-pan-cytokeratin followed by exposure to both secondary antibodies. Some samples of fertilized eggs were exposed for 30 min after methanol fixation to 10 or 20 U of RNase from bovine pancreas (Roche, Mannheim, Germany) in 1× SSC.

An Olympus Fluoview (Olympus, Segrate, Italy) confocal microscope, based on an Olympus IX-70 inverted microscope, was used for all experiments. A Kr/Ar laser was used to produce the excitation laser lines at 488 and 568 nm. Fluorescence emission wavelengths were separated by a 530-nm dichroic mirror followed by passage through a 510- to 550-nm bandpass filter (green fluorescence emission) or a 585-nm longpass filter (red fluorescence emission). Images were then collected in a photomultiplier. Laser power and photomultiplier settings

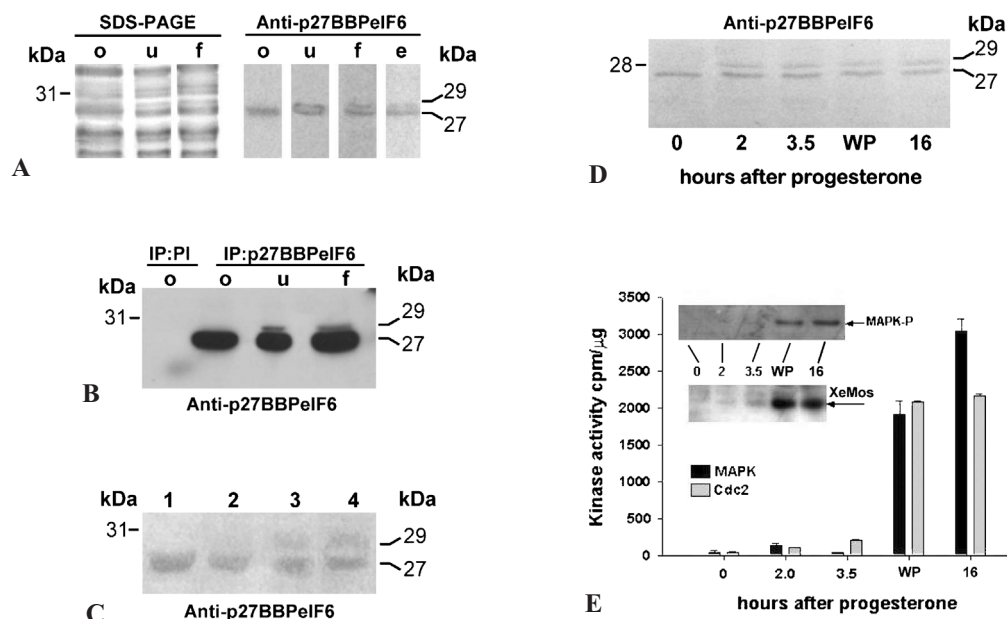


Figure 1. p27^{BBP}/eIF6 distribution in oocytes and in eggs. (A) Left: SDS-PAGE (10% polyacrylamide) of oocytes (o), unfertilized (u) and fertilized (f) egg supernatant. Right: Western blotting with monoclonal anti-p27^{BBP}/eIF6 antibody and AP-conjugated secondary antibodies. A 27-kDa band cross-reacting with the antibody is present in oocytes, unfertilized and fertilized eggs and embryos (neurula) (e). In unfertilized and fertilized eggs and embryos a second band of 29 kDa cross-reacts with the same antibody. (B) Supernatants of oocytes, unfertilized and fertilized eggs immunoprecipitated with anti-p27^{BBP}/eIF6 polyclonal antibodies. The immunoprecipitates were run on 10% polyacrylamide gels, blotted, incubated with the same antibodies and revealed by Protein A-peroxidase-ECL. As control, oocyte supernatant was immunoprecipitated with pre-immune serum (PI). While in the control oocytes, no band was detected, the 27-kDa band was found in the three samples immunoprecipitated by anti-p27^{BBP}/eIF6, and the 29-kDa band was found in the u and f eggs. (C) St. 6 oocytes treated with TPA or progesterone and utilized for SDS-PAGE (15% polyacrylamide) and Western blot with anti-p27^{BBP}/eIF6 and secondary AP-conjugated antibodies. The original gels used for this Western blot were charged with 60 mg for each well and over-run to improve band separation. Lane 1, untreated oocytes; lane 2, TPA exposed oocytes and (lane 3) related control; lane 4, progesterone-exposed oocytes. The 29-kDa band appears in both progesterone- and TPA-exposed oocytes. (D) Western blot of a gel loaded with equal protein amounts of oocytes collected at times 0, 2, 3.5, the white-spot stage (WP) and 16 h following progesterone treatment (M-II). The 29-kDa protein was immunodetected 2 h following progesterone exposure. (E) Kinase activity of MAPK and Cdc2 in oocytes at different time points after progesterone treatment. The same oocyte samples used for the experiments in D were utilized in these assays. At the indicated times after progesterone induction, oocytes were lysed and 20 mg of supernatants assayed to measure Cdc2 and MAP kinase activities (graph). WP, white spot. Alternatively, 40 mg of the same samples was separated on SDS-PAGE, blotted to nitrocellulose and probed with anti-*Xenopus* Mos (XeMos) or anti-phospho-MAP kinase (MAPK-P). Immunoreactivity was detected by ECL plus.

were kept constant for all experiments. Experiments were standardized by using sections spaced at 1- μ m intervals using a $\times 60/1.25$ NA UPlanFl fluorescence objective (Olympus). Images were processed by the confocal software and Adobe Photoshop.

Analysis of confocal images

Confocal images were analyzed to examine the extent of p27^{BBP}/eIF6 along cytokeratin fibres or in the whole cytoplasm. The analysis was performed using the confocal software. Graphs of localization on cytokeratin filaments were analysed by recording green fluorescence along a fibre of cytokeratin traced by the confocal software. Because cytokeratin fibres were of variable lengths, diverse traces were accumulated to form a total of 50 μ m of cytokeratin fibre length. Areas of p27^{BBP}/eIF6 were defined as peaks of green fluorescence greater than 2000 fluorescence units (background fluorescence averaged 500 fluorescence units). For each analysis (a minimum of three samples), ten single confocal sections were superimposed to provide the images used in the analysis. Peaks of p27^{BBP}/eIF6 fluorescence were again recorded over 2000 fluorescence units in an area of interest of the egg cytoplasm, defined by the confocal software analysis program. Here, single confocal slices were used to measure the number of peaks. Where indicated, peripheral areas immediately under the egg plasma membrane were measured and internal areas were measured 40 μ m from the plasma membrane, as visualized by the confocal section.

Results

p27^{BBP}/eIF6 protein is in the oocytes and is modified after progesterone or TPA-induced oocyte maturation

Supernatants of previtellogenic and vitellogenic oocytes (meiotic prophase I), unfertilized eggs (meiotic metaphase II), early zygotes (meiotic telophase II-first cleavage cycle) displayed a band of approximately 27 kDa by SDS-PAGE and Western blotting, using either monoclonal or polyclonal anti-p27^{BBP}/eIF6 antibodies and AP-conjugated secondary antibodies. In unfertilized and fertilized eggs, a second band of about 29 kDa cross-reacted with the same antibodies. The two bands were maintained throughout development to the neurula stage (fig. 1A). Similar results, i.e. the presence of a 27-kDa band and a 29-kDa band, were obtained by immunoprecipitation of total extract of unfertilized eggs and fertilized eggs with anti-p27^{BBP}/eIF6 (fig. 1B). These samples were ECL-developed. We noted that during immunoprecipitation, the 29-kDa band was less efficiently recovered, suggesting differential localization leading to antigenic masking. We hypothesized that the 29-kDa band is a developmentally regulated post-translational modification of p27^{BBP}/eIF6.

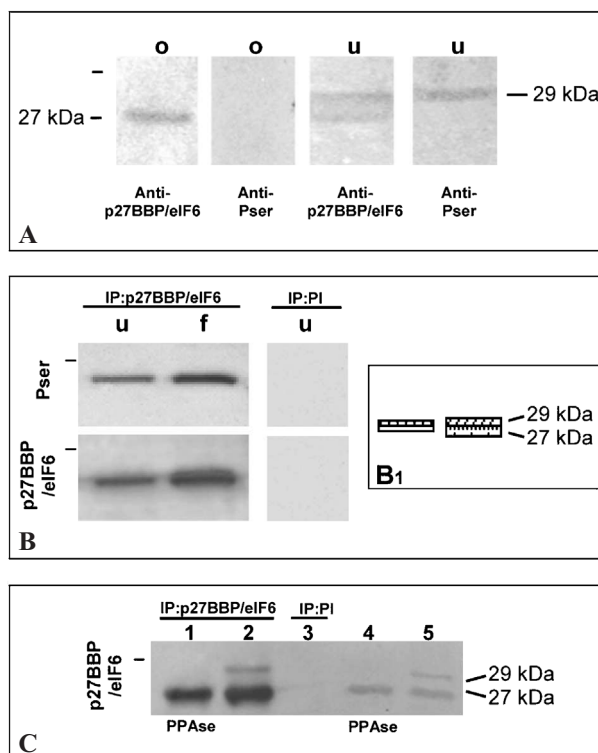


Figure 2. (A) Western blot of oocytes (o) and unfertilized eggs (u) exposed to anti-phosphoserine (anti-Pser) or to anti-p27^{BBP}/eIF6, as indicated, and revealed by AP-conjugated secondary antibodies. In the unfertilized eggs, the 29-kDa band cross-reacts with anti-p27^{BBP}/eIF6 and anti-phosphoserine. B. Western blot of unfertilized (u) and fertilized (f) egg supernatants immunoprecipitated with anti-p27^{BBP}/eIF6 or with preimmune serum. The blot was first incubated with anti-phosphoserine and revealed by protein A-peroxidase-ECL. The same blot, after stripping, was incubated with p27^{BBP}/eIF6 and similarly revealed, showing that the upper part of the band of u and f cross-reacts with anti-phosphoserine, as reconstructed in B1. In B, pre-immune serum-precipitated (PI) unfertilized eggs are also shown as negative control. (C) Western blots of unfertilized egg supernatants immunoprecipitated with anti-p27^{BBP}/eIF6 or with preimmune serum. Following immunoprecipitation, some samples were treated with calf intestinal alkaline phosphatase (PPase). The blotted 15% gel was run over the front line to improve resolution of the 29-kDa protein. The blots were incubated with anti-p27^{BBP}/eIF6 and revealed by protein A-peroxidase-ECL. Lane 1, immunoprecipitate treated with PPase; lane 2, untreated immunoprecipitate; lane 3, Preimmune serum-precipitated sample; lane 4, total lysate treated with PPase; lane 5, untreated total lysate. The small bar on the left panels indicates the 31-kDa Mr standard.

In vitro maturation of st. 6 oocytes was induced by progesterone or TPA (PKC agonist) treatment [32]. Mature oocytes extracted and probed with a monoclonal p27^{BBP}/eIF6 antibody (fig. 1C) showed the 29-kDa band in progesterone- and TPA-stimulated but not in untreated oocytes. To determine at what stage the 29-kDa band appears along the progesterone-induced pathway, hormone-exposed samples were monitored until several hours after 'white-spot' appearance, run in SDS-PAGE and analysed for p27^{BBP}/eIF6 (fig. 1D). Data indicated that the 29-kDa

band was visible already 2 h following progesterone exposure. In aliquots of the same oocyte samples, Mos and MAPK onset, as well as MAPK and Cdc2 activities were determined (fig. 1E). A comparison of figures 1D and 1E shows that the 29-kDa band was found when the maturation markers started to appear and MAPK and Cdc2 activities were at an initial stage, suggesting that p27^{BBP}/eIF6 undergoes a post-translational change during oocyte maturation.

The 29-kDa band cross-reacts with anti-phosphoserine and disappears following phosphatase treatment

Western blotting showed that the 29-kDa band cross-reacted with anti-phosphoserine (fig. 2A) but not with anti-phosphothreonine (data not shown). We immunoprecipitated p27^{BBP}/eIF6 and probed it for phosphoserine. Data showed that the 29-kDa band immunoprecipitated by anti-p27^{BBP}/eIF6 was recognized by phosphoserine antibodies (fig. 2B). Furthermore, the 29-kDa band was not recovered by immunoprecipitation with anti-p27^{BBP}/eIF6, if extracts were previously incubated with phosphatase (fig. 2C). Thus, data suggest that p27^{BBP}/eIF6 is phosphorylated by a PKC pathway during oocyte maturation.

Protein localization varies according to meiotic stage

In toto confocal microscopy of oocytes showed immunostaining both in the whole nucleoplasm and in strings surrounding the nucleoli (fig. 3a, b). In previtellogenic oocytes, the immunostaining was evenly distributed (fig. 3a). In vitellogenic oocytes, anti-p27^{BBP}/eIF6 immunostaining was clearly present in follicle cells, in the macrovilli of the follicle cells and at the oocyte periphery both in the animal and vegetal hemispheres (fig. 3c, d). However, at the final stages of oocyte growth, this protein acquired a rather polarized distribution, like other molecules and organelles [see ref. 18, 33]. In the animal half, small dots of the immunostain were concentrated at the oocyte surface and in a peripheral layer of 15–20 μm , while sparsely distributed in the cytoplasm bulk (fig. 3c, d). In the vegetal hemisphere, p27^{BBP}/eIF6 distribution in the peripheral layer was not evident and the immunofluorescent dots were even less abundant (fig. 3e).

In unfertilized eggs, the immunostain was spread across the cytoplasm from the periphery to the bulk of the cytoplasm in the animal half (fig. 3g, h). Immunofluorescent dots were detected in the vegetal half and surrounded the numerous yolk platelets appearing as pearl strings (arrow in fig. 3i). One hour after fertilization, abundant immunofluorescent dots were found in the animal half. Some of them were concentrated in a fluorescent shell around cytoplasmic organelles, such as yolk platelets (fig. 3k, l). In the vegetal half, the fluorescence pattern was similar, although dots were sparsely present in the cytoplasm (fig. 3m, n). The immunostaining was specific (fig. 3f, j).

p27^{BBP}/eIF6 binds 60S subunits, partially overlaps with cytokeratin and is functionally linked to the CSK

In mammalian cells, p27^{BBP}/eIF6 is associated with the CSK. In addition, in yeasts and mammals, it is partially linked to 60S ribosomal subunits [1, 2, 5]. In *Xenopus*, immunoprecipitation of p27^{BBP}/eIF6 leads to co-precipitation of ribosomal protein L5 (fig. 4a), suggesting that, at least part of p27^{BBP}/eIF6 is bound to 60S subunits. Similarly, in ribosome profiles, p27^{BBP}/eIF6 sedimented with the ribosomes, peaking at 60S–80S, was absent on polysomes and was present in the soluble phase (fig. 4b). Since this analysis excludes cytoskeletal bound p27^{BBP}/eIF6, we conclude that p27^{BBP}/eIF6 is present on 60S, absent from polysomes (as in yeasts and mammals), but also present in other compartments (soluble and insoluble).

To gain information about the CSK association of p27^{BBP}/eIF6, which eludes ribosomal analysis, samples were incubated with anti-cytokeratin and anti-p27^{BBP}/eIF6 antibodies and observed by confocal microscopy. In st. 6 oocytes, some overlap of fluorochromes was recorded in the follicle cells and oocyte membranes and in the surrounding thecae. Furthermore, anti-p27^{BBP}/eIF6-stained dots were found mostly in the peripheral cytoskeletal network delimited by bundles cross-reactive with anti-cytokeratin antibodies (fig. 5a). Figure 5b is a control section where staining is absent. In unfertilized eggs, practically no overlap was observed of the two antibodies (fig. 5c). In the animal halves of fertilized eggs, cytokeratin was organized in short bundles immersed in the cytoplasm. Figure 5d indicates contiguity or overlap between cytokeratin and p27^{BBP}/eIF6, particularly around the yolk platelets. In corresponding vegetal halves (fig. 5e, f), the thick bundles of cytokeratin were spread across the zygote periphery and co-localized with p27^{BBP}/eIF6. The protein was spot-like and decorated the cytokeratin bundles, acquiring a yellow fluorescence (BODIPY FL and Texas Red fluorescence), in contrast to the green fluorescence (BODIPY FL-labelling) of p27^{BBP}/eIF6 dispersed in the cytoplasm (fig. 5f). A frequency trace of the p27^{BBP}/eIF6 localization on cytokeratin fibres in oocytes and fertilized eggs is shown in figure 5i (I, II, III). In samples treated with 20 U RNase (fig. 5g, h), sites of co-localization appeared to be sparser than in the untreated eggs. Indeed, comparison of the frequency trace of RNase-treated fertilized eggs versus the trace of corresponding untreated samples strongly suggests that the sites of co-localization decreased following RNase treatment (compare fig. 5i IV, with 5i II and III). In this sense, p27^{BBP}/eIF6 fluorescence peaks were higher in control images than in RNase-treated samples, with no distinction between the peripheral and the internal cytoplasm (table 1).

In cleaving embryos, cytokeratin and p27^{BBP}/eIF6 were mixed in the cytoplasm and appeared to colocalize in particular at the blastomere periphery (fig. 6a). In embryos exposed to cytochalasin B at the two-cell stage, we found

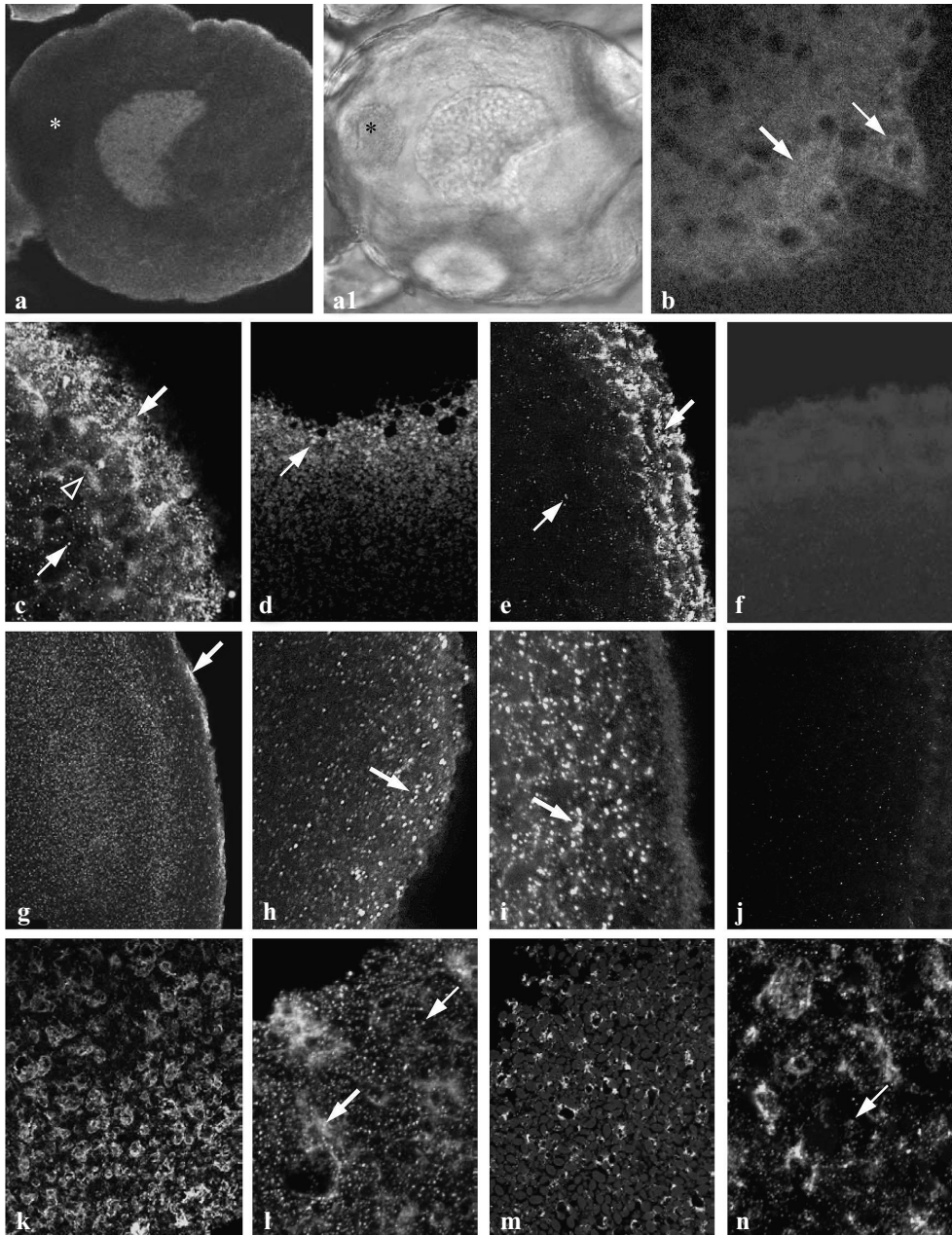


Figure 3. Confocal immunolocalization of p27^{BBP}/eIF6 in oocytes and unfertilized and fertilized eggs with BODIPY-conjugated secondary antibodies. Each image was elaborated using three optical sections 1- μ m thick. Stage 2 oocyte showing a general cross-reactivity to the antibody in the germinal vesicle (a) that is evident in thin chains (b, large arrow) that surround nucleoli (small arrow). The mitochondrial cloud is indicated with an asterisk (a) and in the corresponding phase contrast image (a1): it is not immunoreactive. a, a1, $\times 230$; b $\times 1000$. (c) Tangential view of the animal hemisphere of a st. 5 oocyte. The large arrow points to the theca and follicle cells whose boundaries are immunoreactive. The arrowhead indicates the articulated peripheries of the oocyte and the follicle cells that are cross-reactive, similar to the small dots in the peripheral cytoplasm (small arrow); $\times 500$. (d) Animal half of an oocyte where the somatic cells were removed. The immunoreactive dots (small dots) are present in a layer of 15–20 μ m; $\times 500$. (e) Vegetal half of the same oocyte shown in c, where the large arrow points to the somatic tissue and the small arrow to the sparse immunoreactive dots in the peripheral cytoplasm; $\times 500$. (f) Control image of the vegetal half of the oocyte where no staining is present; $\times 500$. (g) Optical section of the animal hemisphere taken at the equator of an unfertilized egg. The immunofluorescence is relevant at the egg periphery (large arrow) and is also widespread in the rest of the cytoplasm; $\times 70$. (h) The animal half periphery shows a high concentration of immunoreactive dots that may fuse together (large arrow); $\times 850$. (i) Vegetal half of the same egg as in h, showing that the immunoreactive dots form a string of pearls around organelles such as yolk platelets (large arrow); $\times 850$. (j) Control image of an egg animal half: the immunostain is absent; $\times 850$. (k) Tangential view of the animal hemisphere of a fertilized egg, showing an immunoreactive rim around cytoplasmic organelles, $\times 300$. At a higher magnification (l) ($\times 1000$) in addition to the fluorescence around the organelles (large arrow), immunoreactive dots are abundantly present (small arrow). (m, n) Corresponding views of the vegetal side of the fertilized egg where the immunoreactive dots (small arrow) are less concentrated than in the animal half (compare l with n). m $\times 300$, n, $\times 1000$.

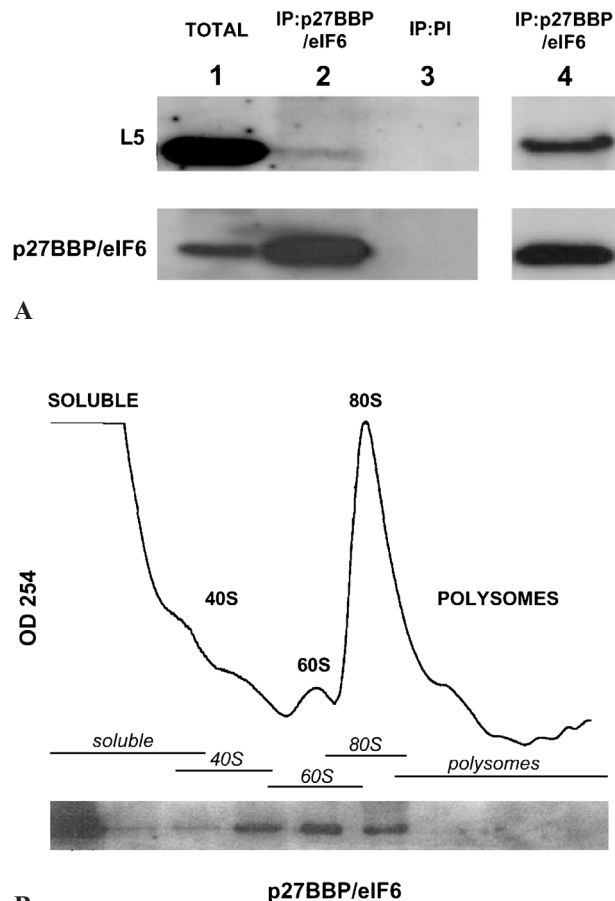


Figure 4. p27^{BBP}/eIF6 association with ribosomes. (A) Oocyte supernatant immunoprecipitated with anti-p27^{BBP}/eIF6, blotted and incubated with anti-L5 or anti-p27^{BBP}/eIF6, as indicated. The blots were ECL-revealed. 1, stage 4–6 oocytes total supernatant; 2, anti-p27^{BBP}/eIF6-immunoprecipitated oocyte supernatant; 3, oocyte supernatant immunoprecipitated with preimmune serum; 4, anti-p27^{BBP}/eIF6-immunoprecipitated A431 mammalian cells, as positive control. On the anti-p27^{BBP}/eIF6-immunoprecipitated supernatant of oocytes (2), a band immunoreactive with anti-L5 is detectable. (B) Sucrose gradient analysis. Fractions from unfertilized eggs were separated on 15–50% sucrose gradients. Gradient fractions were collected while the optical density profile at 254 nm was monitored (upper panel). Aliquots of each fraction were used for immunoblotting with anti-p27^{BBP}/eIF6 (lower panel).

Table 1. Distribution of p27^{BBP}/eIF6 after RNase treatment of fertilized eggs.

	No RNase	RNase	<i>p</i>
Periphery	0.77 ± 0.12 (n = 60)	0.4 ± 0.02 (n = 60)	<0.001
Internal	0.39 ± 0.01 (n = 60)	0.23 ± 0.04 (n = 60)	<0.001

Values represent the mean ± SD of peaks of green fluorescence per 100 μm² of cytoplasm. Data were collected using ten analyses of at least three separate experiments. Internal regions are 40 μm inside the egg cytoplasm.

that, as expected, the cleaving furrows had disappeared (fig. 6b). Here, the cytokeratin localization was strongly affected, being located mostly at the embryo periphery. p27^{BBP}/eIF6 followed this distribution (fig. 6b). In an optical section taken from the equator, in the animal half, the finely intermingled co-localization of both proteins at the cell periphery could be observed (fig. 6c). Figure 6d is a control sample where the immunostain is absent.

Taken together, the data indicate that p27^{BBP}/eIF6 associates with the CSK according to the developmental stage. In addition, association with the CSK is impaired by RNase treatment (see Discussion).

Discussion

We studied p27^{BBP}/eIF6 localization and post-translational modifications during oogenesis and early embryonic stages in *X. laevis*. Three properties have been described in the past for p27^{BBP}/eIF6: association with 60S and ribosomes in yeasts and mammals [4, 2]; PKC-dependent modifications coincident with translation in human cancer [5]; association with intermediate filaments in mammalian cells [1, 34]. We observed that these properties are also present in *Xenopus*. However, our data, the first in an in vivo multicellular and developing system, suggest that these properties are developmentally regulated.

The association of p27^{BBP}/eIF6 with ribosomes has been observed in yeasts and mammals. Here we confirm findings from these systems. Importantly, we observe that p27^{BBP}/eIF6 is excluded from polysomes in line with the notion that p27^{BBP}/eIF6 must be released from 60S to start translation [see ref. 5]. Additionally, we noted that, unlike yeasts, the amount of p27^{BBP}/eIF6 not bound to ribosomes is higher [see ref. 5]. This observation suggests that during evolution, p27^{BBP}/eIF6 may have acquired novel functions. We observe for the first time in vivo a developmental change of p27^{BBP}/eIF6 electrophoretic mobility. In vitro maturation experiments coupled with Western blotting showed that, upon oocyte stimulation by progesterone, a major post-translation change of p27^{BBP}/eIF6 takes place, i.e. a higher-Mr band of 29 kDa appears, as a result of its de novo serine phosphorylation. The 29-kDa band is also observed in developing embryos, indicating that it is produced as well by the zygotic genome. One interesting possibility is that the kinase involved is PKC as shown in mammalian cells [5] and this may have a major functional role in oocyte maturation. In *Xenopus* oocytes, progesterone is known to act synergistically to [35] or via [9] PKC. In this work, the 29-kDa protein appears before the ‘white-spot’ stage, suggesting that during oogenesis, p27^{BBP}/eIF6 phosphorylation occurs at the onset of the major Mos/MPF activation events. No direct evidence is yet available that the observed phosphorylation in serine is caused by PKC. However, the fact that the 29-kDa pro-

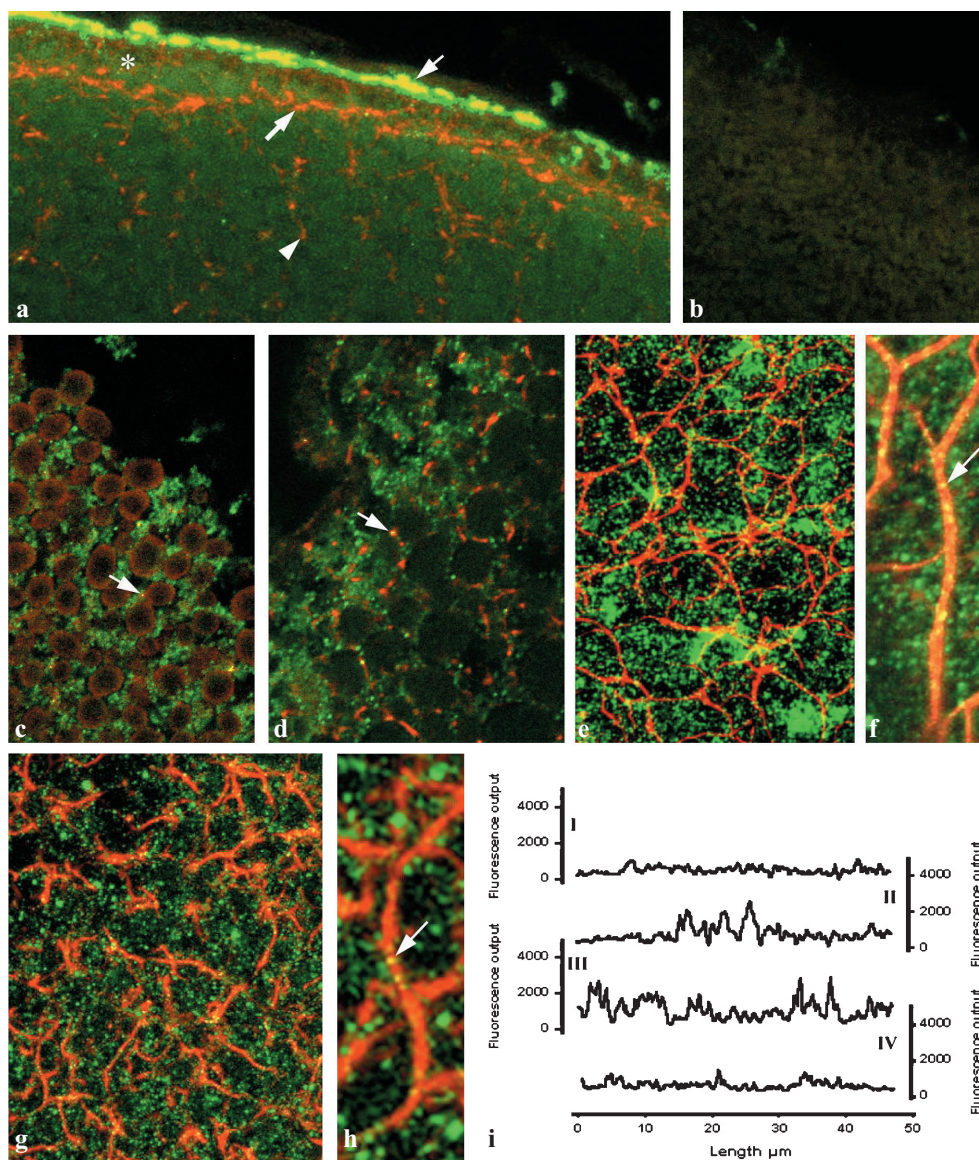


Figure 5. Confocal immunoco-localization of p27^{BBP}/eIF6 and cytokeratin in st. 6 oocytes and unfertilized and fertilized eggs. The secondary antibodies were BODIPY-conjugated anti-rabbit goat IgG for anti-p27^{BBP}/eIF6 and Texas Red-conjugated anti-mouse goat antibodies for anti-pan cytokeratin. Images were elaborated as indicated in figure 4. (a) Animal half of a st. 6 oocyte. Note a co-localization of both antibodies in the somatic tissue (small arrow). Anti-p27^{BBP}/eIF6-stained dots (asterisk) are embedded in the peripheral network of the CSK delimited by anti-cytokeratin antibody-stained fibres (large arrow). The arrowhead shows the 'radii' of the CSK where no co-localization was found with anti-p27^{BBP}/eIF6 antibodies. $\times 350$ (b) Control st. 6 oocyte, incubated with pre-immune serum. The staining is absent. $\times 350$. (c) Animal half of an unfertilized egg, at the equator. The cytoplasmic organelles are surrounded by an anti-cytokeratin cross-reacting ring (in red), where little or no co-localization (in yellow) with anti-p27^{BBP}/eIF6 (in green) is present (small arrow). $\times 1000$. (d) Animal half of a fertilized egg, at the equator. Cytokeratin surrounds the organelles as short bundles where some co-localization (in yellow) of the two antibodies occurs (arrow). $\times 1200$. (e) Vegetal half of a fertilized egg. The optical section shows the conspicuous peripheral cytoskeletal network that forms in this region following fertilization. $\times 1100$. (f) Higher magnification of the vegetal half of a fertilized egg. A dot-like localization of p27^{BBP}/eIF6 is spread throughout the cytoplasm, on the cytokeratin-containing fibres (arrow) and on the thinner CSK network branching from the large one. $\times 1700$. (g) Vegetal half of a fertilized egg, treated with 20 U RNase. $\times 1100$. (h) Detail of the sample shown in g. Little co-localization of p27^{BBP}/eIF6 and cytokeratin is seen (arrow). $\times 1700$. (a-h) Each figure was elaborated using 15 optical sections. (i) Graphs are a representative example of the confocal green fluorescence (p27^{BBP}/eIF6) output measured by following a trace of cytokeratin fibres (red fluorescence). The top trace (I) shows the periphery of the animal half of the oocyte, the central trace (II) is the periphery of the animal half of the fertilized egg and the lower trace (III) is the periphery of the vegetal half of the fertilized egg. IV is a trace of green fluorescence along a cytokeratin fiber after treatment of fertilized eggs (vegetal half) with 20 U RNase. The trace is recorded in an area 40 μm from the periphery of the egg. All traces are measured along a total of 50 μm cytokeratin fibres.

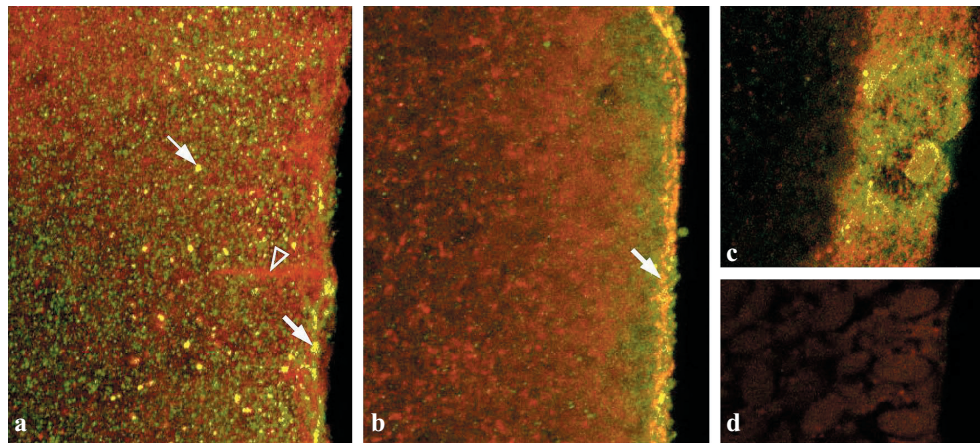


Figure 6. Confocal immunocolocalization of p27^{BBP}/eIF6 and cytokeratin in cytochalasin B-treated embryos. The secondary antibodies were the same as indicated for figure 5. Images were elaborated as indicated in figures. 3 and 5. (a) Untreated cleaving embryo, animal side, at the equator. Cytokeratin and p27^{BBP}/eIF6 appear to co-localize both at the blastomere membranes (large arrow) and in the cytoplasmic dots (small arrow). Arrowhead cleavage furrow. $\times 900$; (b) Cognate embryo where cleavage could not occur as a consequence of cytochalasin B exposure. The optical section was taken at the embryo equator. Most p27^{BBP}/eIF6 is at the membrane, where co-localization with cytokeratin is evident (arrow). $\times 760$. (c) Detail of the co-localization of cytokeratin and p27^{BBP}/eIF6 in a tangential view of a cytochalasin B-treated embryo. $\times 900$. (d) Control sample of cleaving embryo. The immunostain is absent. $\times 900$.

tein is produced in the oocyte by TPA treatment argues in favour of this hypothesis. Furthermore, in *Xenopus*, two potential PKC phosphorylation sites in Ser were found in p27^{BBP}/eIF6 cDNA [M. C. Vaccaro et al., unpublished data]. In vitro and in cancer cells, PKC-mediated phosphorylation of p27^{BBP}/eIF6 is part of the major biological role of p27^{BBP}/eIF6 in mammals. In fact, PKC-mediated phosphorylation of p27^{BBP}/eIF6 results in its release from 60S and translation [5]. Data in this paper suggest the first example where phosphorylation of p27^{BBP}/eIF6 is functional to the regulation of translation along a developmental pathway. Indeed, p27^{BBP}/eIF6 phosphorylation of *X. laevis* oocytes occurs following removal of the meiotic translation block at maturation, a time when the regulation of protein synthesis is orchestrated by new mechanisms [36]. Accordingly, we found a higher concentration of immunofluorescent dots, in the animal half compared to the vegetal half after fertilization, and the activity in protein synthesis of the animal half is higher than in the vegetal half of *Xenopus* fertilized eggs [37]. Moreover, the coalesced configuration of p27^{BBP}/eIF6 around cytoplasmic organelles and its co-localization with the CSK occur after maturation, when the phosphorylated and the unphosphorylated forms of p27^{BBP}/eIF6 are both present throughout the cytoplasm and the cytoskeleton is sharply rearranged [see ref. 20]. In contrast, in the oocyte at prophase arrest, when only the unphosphorylated form is found, confocal microscopy showed that p27^{BBP}/eIF6 colocalizes with the CSK in the follicle cells but not with the oocyte cytoplasmic CSK [see ref. 18]. Indeed, in the animal half, p27^{BBP}/eIF6 is segregated in a layer, intermingled but not co-localizing with a cytoskeletal network located therein [18, 19].

In yeast, phosphorylation in serine of Tif6p, the homologue of p27^{BBP}/eIF6, by casein kinase 1 was found to regulate p27^{BBP}/eIF6 nucleocytoplasmic distribution [38], suggesting that this event may be similarly involved in regulating protein distribution in *Xenopus* oocytes. This event being mediated by casein kinase 1, it is unlikely to reflect the PKC-stimulated appearance of the 29-kDa band, although further studies would be required to reach a definitive conclusion.

The p27^{BBP}/eIF6 co-localization with the CSK filament network is, strikingly, developmentally regulated. It occurs in fertilized eggs over spots aligned along the bundle axis, while dots reactive uniquely with anti-p27^{BBP}/eIF6 are spread throughout the cytoplasm. Cytochalasin B experiments and confocal microscopy suggest a functional association of p27^{BBP}/eIF6 with the CSK. On the other hand, RNase depletion of the anti-p27^{BBP}/eIF6-reacting spots on cytokeratin fibres, as indicated by fluorescence frequency analysis, strongly suggests that some of the p27^{BBP}/eIF6 is linked to RNA bound to those fibres. One should note that, in our experiments, enzymatic treatment is apparently effective in removing p27^{BBP}/eIF6 also from RNase-sensitive sites throughout the cytoplasm. The actual role of p27^{BBP}/eIF6 binding to the CSK is unclear, especially where $\beta 4$ integrin is absent. We propose the following hypothesis. In eukaryotic cells, the majority of mRNAs and polyribosomes have been shown to be associated with the cytoskeleton [reviewed in ref. 39]. In cell-free extracts, 40S and 60S ribosomes bind to intermediate filaments at the N-terminal head domain of cytokeratin [40, 41]. As p27^{BBP}/eIF6 binds to 60S in eukaryotic cells [2], the intriguing possibility exists that p27^{BBP}/eIF6 on cytokeratin filaments observed in this study indicates

sites where p27^{BBP}/eIF6 binds to 60S, forming 60S-p27^{BBP}/eIF6 complexes. If this is correct, then in early embryogenesis, 60S-p27^{BBP}/eIF6 may be stored at the cytoskeleton and made available for use according to cellular needs. Ceci et al. [5] showed that p27^{BBP}/eIF6 binds to the 60S subunits when it is not phosphorylated by PKC. Therefore the cyokeratin-linked RNA-p27^{BBP}/eIF6 complexes may represent a storage of inactive 60S in *Xenopus* eggs. Our next step will be to analyse cyokeratin-p27^{BBP}/eIF6 binding under various experimental conditions.

Acknowledgements. We are grateful to G. Falcone for image processing and to V. Monfrecola for technical assistance. This work was supported by a PRIN grant to C. C., S. B and P. C. M and by an ABCD fellowship to N. D. M. This study was carried out under the auspices of the Italian MIUR Centre of Excellence in Physiopathology of Cell Differentiation (PCM).

- Biffo S., Sanvito F., Costa S., Preve L., Pignatelli R., Spinardi L. et al. (1997) Isolation of a novel $\beta 4$ integrin binding protein (p27^{BBP}) highly expressed in epithelial cells. *J. Biol. Chem.* **272**: 30314–30321
- Sanvito F., Piatti S., Villa A., Bossi M., Lucchini G., Marchisio P. C. et al. (1999). The $\beta 4$ integrin interactor p27^{BBP}/eIF6 is an essential nuclear matrix protein involved in 60s ribosomal subunit assembly. *J. Cell Biol.* **144**: 823–838
- Basu U., Si K., Warner J. R. and Maitra U. (2001) The *Saccharomyces cerevisiae* TIF6 gene encoding translation initiation factor 6 is required for 60S ribosomal subunit biogenesis. *Mol. Cell. Biol.* **21**: 1453–1462
- Si K. and Maitra U. (1999). The *Saccharomyces cerevisiae* homologue of mammalian translation initiation factor 6 does not function as a translation initiation factor. *Mol. Cell. Biol.* **19**: 1416–1426
- Ceci M., Gaviraghi C., Gorrini C., Marchisio P. C. and Biffo S. (2003). Assembly of 80S ribosomes requires phosphorylation-dependent release of p27^{BBP}/eIF6 from 60S subunits. *Nature* **426**: 580–584
- Senger B., Lafontaine D. L., Graindorge J. S., Gadala O., Camasses A., Sanni A. et al. (2001). The nucleolar Tif6p and Efl1p are required for a late cytoplasmic step of ribosome synthesis. *Mol Cell.* **8**: 1363–1373
- De Simone D. W. and Hynes R. O. (1988). *Xenopus laevis* integrins: structural conservation and evolutionary divergence of integrin beta subunits. *J. Biol. Chem.* **263**: 5333–5340
- Capco D. G., Tutnick J. M. and Bement W. M. (1992). The role of protein kinase C in reorganization of the cortical cytoskeleton during the transition from oocyte to fertilization-competent egg. *J. Exp. Zool.* **264**: 395–405
- Johnson J. and Capco D. G. (1997). Progesterone acts through protein kinase C to remodel the cytoplasm as the amphibian oocyte becomes the fertilization-competent egg. *Mech. Dev.* **67**: 215–226
- Bouvet P. and Wolffe A. P. (1994). A role for transcription and FRGY2 in masking maternal mRNA within *Xenopus* oocytes. *Cell* **77**: 931–941
- Stutz A., Conne B., Huarte J., Gubler P., Volkel V., Flandin P. et al. (1998). Masking, unmasking and regulated polyadenylation cooperate in the translational control of a dormant mRNA in mouse oocytes. *Genes Dev.* **12**: 2535–2548
- Richter J. D. (1999). Cytoplasmic polyadenylation in development and beyond. *Microbiol. Mol. Biol. Rev.* **63**: 446–456
- Moor C. H. de and Richter J. D. (1999). Cytoplasmic polyadenylation elements mediate masking and unmasking of cyclin B1 mRNA. *EMBO J.* **18**: 2294–2903
- Mendez R., Barnard D. and Richter J. D. (2002). Differential mRNA translation and meiotic progression require Cdc2-mediated CPEB destruction. *EMBO J.* **21**: 1833–1844.
- Davidson E. H. (1986). *Gene Activity in Early Development*. 3rd ed., Academic Press, New York
- Bremer J. W., Busich H. and Yeoman L. C. (1981) Evidence for a species of nuclear actin distinct from cytoplasmic and muscle actins. *Biochemistry* **20**: 2013–2017
- Carotenuto R., Maturi G., Infante V., Capriglione T., Petrucci T. and Campanella C. (1997). A novel protein cross-reacting with antibodies against spectrin is localized in the nucleoli of amphibian oocytes. *J. Cell Sci.* **110**: 2683–2690
- Gard D. L., Cha B. J. and King E. (1997). The organization and animal-vegetal asymmetry of cyokeratin filaments in stage 6 *Xenopus* oocytes is dependent upon F-actin and microtubules. *Dev. Biol.* **184**: 95–114
- Gard D. L. and Klymkowsky M. W. (1998). Intermediate filament organization during oogenesis and early development of the clawed frog, *Xenopus laevis*. In: *Subcellular Biochemistry*, vol. 31: Intermediate Filaments, pp. 35–70. Herman H. and Harris W. A. (eds), Plenum, New York
- Klymkowsky M. W., Maynell L. A. and Polson A. G. (1987). Polar asymmetry in the organization of the cortical cyokeratin system of *Xenopus laevis* oocytes and embryos. *Development* **100**: 543–557
- Klymkowsky M. W. and Maynell L. A. (1989). MPF-induced breakdown of cyokeratin filament organization in the maturing *Xenopus* oocyte depends upon the translation of maternal mRNAs. *Dev. Biol.* **134**: 479–485
- Klymkowsky M. W., Maynell L. A. and Nislow C. (1991). Cyokeratin phosphorylation, cyokeratin filament severing and the solubility of the maternal Vg1. *J. Cell Biol.* **114**: 787–797
- Klymkowsky M. W. and Karnovsky A. (1994). Morphogenesis and the cytoskeleton: studies of the *Xenopus* embryo. *Dev. Biol.* **165**: 372–348
- Nadano D, Ishihara G., Aoki C, Yoshinaka T., Irie S. and Sato T. A. (2000). Preparation and characterization of antibodies against human ribosomal proteins: heterogeneous expression of S11 and S30 in a panel of human cancer cell lines. *Jpn. J. Cancer Res.* **9**: 802–810
- Franz J. K. and Franke W. W. (1986). Cloning of cDNA and amino acid sequence of a cyokeratin expressed in oocytes of *Xenopus laevis*. *Proc. Natl. Acad. Sci. USA.* **83**: 6475–6479.
- Maturi G., Infante V., Carotenuto R., Focarelli R., Caputo M. and Campanella C. (1998). Specific glycoconjugates are present at the oolemma of the fertilization site in the egg of *Discoglossus pictus* (Anurans) and bind spermatozoa in an in vitro assay. *Dev. Biol.* **204**: 210–223
- Campanella C., Andreuccetti P., Taddei C. and Talevi R. (1984). The modifications of cortical endoplasmic reticulum during 'in vitro' maturation of *Xenopus laevis* oocytes and its involvement in cortical granule exocytosis. *J. Exp. Zool.* **229**: 283–294
- Tunquist B. J. and Maller J. L. (2003). Under arrest: cyostatic factor (CSF)-mediated metaphase arrest in vertebrate eggs. *Genes Dev.* **17**: 683–710
- Russo G., Kyozuka K., Antonazzo L., Tosti E. and Dale B. (1996). Maturation promoting factor in ascidian oocytes is regulated by different intracellular signals at meiosis I and II. *Development* **122**: 1995–2003
- Bluemink J. G. (1978). Use of cytochalasins in the study of amphibian development. *Front. Biol.* **46**: 113–142
- Cardinali B, Carissimi C, Gravina P and Pierandrei-Amaldi P. (2003). La protein is associated with terminal oligopyrimidine mRNAs in actively translating polysomes. *J Biol Chem.* **278**: 35145–35151
- Stith B. J. and Maller J. L. (1987). Induction of meiotic maturation in *Xenopus* oocytes by 12-O-tetradecanoylphorbol 13 acetate. *Exp. Cell Res.* **169**: 514–523

- 33 Carotenuto R., Vaccaro M. C., Capriglione T., Petrucci T. C. and Campanella C. (2000) Alpha-spectrin has a stage-specific asymmetrical localization during *Xenopus* oogenesis. *Mol. Reprod. Dev.* **55**: 229–239
- 34 Ceci M., Offenhauser N., Marchisio P. C. and Biffo S. (2002). Formation of nuclear matrix filaments by p27 BBP/eIF6. *Biochem. Biophys. Res. Commun.* **295**: 295–299
- 35 Stith J. B., Goalstone M. L. and Kirkwood A. J. (1992). Protein kinase C initially inhibits the induction of meiotic cell division in *Xenopus* oocytes. *Cell Signal.* **4**: 393–403
- 36 Ovsenek N., Zorn A. M. and Krieg P. A. (1992). A maternal factor, OZ-1, activates embryonic transcription of the *Xenopus laevis* gene. *Development* **115**: 649–655
- 37 Bement W. M. and Capco D. G. (1989). Activators of protein kinase C trigger cortical granule exocytosis, cortical contraction, and cleavage furrow formation during egg activation. *J. Exp. Zool.* **263**: 219–242
- 38 Basu U., Si K., Deng H. and Maitra U. (2003). Phosphorylation of mammalian eukaryotic translation initiation factor 6 and its *Saccharomyces cerevisiae* homologue Tif6p regulates its nucleoplasmic distribution and is required for yeast cell growth. *Mol. Cell. Biol.* **23**: 6186–6199
- 39 Hesketh J. E. (1996). Sorting messenger RNAs in the cytoplasm: mRNA localization and the cytoskeleton. *Exp. Cell Res.* **225**: 219–236
- 40 Bauer C. and Traub P. (1995). Interaction of intermediate filaments with ribosomes in vitro. *Eur. J. Cell Biol.* **68**: 288–296
- 41 Wang Q., Tolstonog G. V., Shoeman R. and Traub P. (2001). Sites of nucleic acid binding in type I–IV intermediate filament subunit proteins. *Biochem.* **40**: 10342–10349



To access this journal online:
<http://www.birkhauser.ch>
